JPET Fast Forward. Published on August 13, 2018 as DOI: 10.1124/jpet.118.250142
This article has not been copyedited and formatted. The final version may differ from this version.

Title Page

Induced pluripotent stem cell derived podocyte like cells as models for assessing mechanisms underlying heritable disease phenotype: initial studies using two Alport syndrome patient lines indicate impaired potassium channel activity

John M. Haynes, James N. Selby, Teresa H. Vandekolk, Isaiah PL. Abad, Joan K. Ho, Wai-Ling Lieuw, Katie Leach, Judith Savige, Sheetal Saini, Craig L. Fisher & Sharon D. Ricardo

Monash Institute of Pharmaceutical Sciences, Monash University, Victoria, Australia (J.M.H., J.N.S., T.H.V., I.P.L.A., J.K.H., W.L., K.L.). Department of Medicine, Royal Melbourne Hospital (J.S.) Department of Anatomy and Developmental Biology, Monash University, Victoria, Australia (S.S., C.L.F., S.D.R.).

Running Title Page

Running title: Function in pluripotent stem cell derived podocyte-like cells

Author for correspondence: John M. Haynes

Monash Institute of Pharmaceutical Sciences, Monash University, Victoria.

tel: 613 69903 9072

email: john.haynes@monash.edu

This manuscript consists of

23 pages of text

0 Tables

10 Figures

66 References

Abstract 236 words

Introduction 661 words

Discussion 1527 words

Nonstandard Abbreviations

AS; Alport Syndrome. NHMC; normal human mesangial cell. HIP; human immortalized podocyte-like. KCNMA1; large conductance potassium channel. CaSR; calcium sensing receptor. MEF; mouse embryonic fibroblast. iPS; induced pluripotent stem cell. WT-1; Wilm's tumor-1.

Section assignment: Cellular and Molecular

JPET Fast Forward. Published on August 13, 2018 as DOI: 10.1124/jpet.118.250142
This article has not been copyedited and formatted. The final version may differ from this version.

Abstract

Renal podocyte survival depends upon the dynamic regulation of a complex cell architecture that links glomerular basement membrane to integrins, ion channels and receptors. Alport syndrome is a heritable chronic kidney disease where mutations in α3, α4 or α5 collagen genes promote podocyte death. In rodent models of renal failure, activation of the calcium sensing receptor (CaSR) can protect podocytes from stress related death. In this study we assess CaSR function in podocyte-like cells from induced-pluripotent stem cells derived from two patients with Alport Syndrome (AS1 & AS2), a renal disease free individual (NHMC) and an immortalized podocyte-like (HIP) cell line. Extracellular calcium elicited concentration-dependent elevations of intracellular calcium in all podocyte-like cells. NHMC and HIP, but not AS1 or AS2 podocyte-like cells also showed acute reductions in intracellular calcium prior to elevation. In NHMC podocyte-like cells this acute reduction was blocked by the large conductance potassium channel (KCNMA1) inhibitors iberiotoxin (10nM) and tetraethylammonium (5 mM), as well as the focal adhesion kinase inhibitor PF562271 (10nM). Quantitative PCR and immunolabelling showed the presence of KCNMA1 transcript and protein in all podocyte-like cells tested. Cultivation of AS1 podocytes on decellularized plates of NHMC podocyte-like cells partially restored acute reductions in intracellular calcium in response to extracellular calcium. We conclude that the AS patient-derived podocyte-like cells used in this study show dysfunctional integrin signalling and potassium channel function which may contribute to podocyte death seen in Alport syndrome.

Introduction:

Podocytes regulate renal filtration through slit diaphragms; modified adherens junctions that span the 30-50nm wide gaps between foot processes, with a zipper-like pattern of transmembrane proteins, including nephrin and fatty acid transporter tumor suppressor homologue, and P-cadherin (Reiser et al., 2000). At the cytoplasmic surface, the slit diaphragm contains dense regions of Triton-X resistant material(Mundel and Kriz, 1995), which acts as a signalling hub for downstream regulators of integrin activity, such as focal adhesion kinase(Blattner and Kretzler, 2005), as well as ion channels and G-protein coupled receptors(Greka and Mundel, 2012).

Chronic kidney disease may arise secondary to other diseases, such as diabetes or, less commonly through mutations of genes essential for normal kidney function; such as α-actinin-4(Obeidova et al., 2006) or collagen IV(Feingold et al., 1985). Alport Syndrome (AS) is a genetic condition associated with progressive loss of kidney function as well as hearing loss and eye abnormalities. Individuals with AS have mutations in the *COL4A3*, *COL4A4* or *COL4A5* collagen genes, resulting in the absence of α3α4α5 collagen chains in the glomerular basement membrane. Ultimately AS results in proteinuria and renal failure(Feingold et al., 1985; Barker et al., 1990; Mochizuki et al., 1994; Hudson et al., 2003; Cosgrove, 2011). Although the mechanisms underlying renal failure are unclear, evidence suggests that the translation of mutant *COL4A5* mRNA results in a protein that is unable to interact with heat shock protein 47, an endoplasmic reticulum protein that regulates appropriate protein folding(Ishida and Nagata, 2011). This is thought to lead to incorrectly folded protein accumulation in the endoplasmic reticulum and induction of the unfolded protein response(Pieri et al., 2014).

Although treatments for AS commonly rely on inhibition of effects of angiotensin II to promote podocyte survival, the activation of another G-protein coupled receptor, the calcium sensing

receptor (CaSR) has profound podocyte cytoskeleton-stabilizing and pro-survival effects (Oh et al., 2011).

The paucity of treatments for chronic kidney diseases such as AS is, we believe, partly due to a lack of robust, *in vitro* model systems to study podocyte function in health and disease. Current model systems such as primary cultures of human podocytes only replicate for a short time and cannot be maintained over long periods (Shankland et al., 2007). Alternatively, immortalizing podocytes has enabled the production of large numbers of podocyte-like cells, however, the process of immortalization reduces their suitability for toxicological screening applications and may introduce changes in phenotype that are not immediately obvious. Recently, we have used induced pluripotent stem (iPS) cells, derived from normal human mesangial cells (NHMC) to generate podocyte-like cells that express the morphological and genetic characteristics of human podocytes (Song et al., 2011; Song et al., 2012). The current study extends this work to produce two new AS patient-derived iPS cell lines (AS1 and AS2). Given the contributions of the CaSR (Ogata et al., 2003; Oh et al., 2011) and angiotensin II (Liebau et al., 2006) receptor subtypes to podocyte function and survival, we now use activators of these receptor signalling systems to compare the functional activities of AS and NHMC podocyte-like cells against commonly used human immortalized podocyte-like (HIP) cells(Saleem et al., 2002). We show that AS patient-derived podocyte-like cells show a distinct pattern of response to the addition of activators of the CaSR. In NHMC and HIP, but not AS podocyte-like cells, extracellular calcium-dependent elevations of intracellular calcium are preceded by acute reductions in intracellular calcium. The large conductance calcium activated potassium (KCNMA1) channel opener, NS1619(Olesen et al., 1994), similarly reduced resting calcium in HIPs and NHMC, but not AS podocyte-like cells. In contrast to functional analysis, KCNMA1 channel mRNA and immunolabelled protein were

equally evident in both AS and NHMC podocyte-like cells. Replating AS1 podocytes onto decellularized NHMC podocyte-like cell plates partially restored the acute reductions in intracellular calcium. We conclude that the two AS patient-derived podocyte-like cell lines generated herein show a loss of large KCNMA1 channel activity, and speculate that the loss of function of these channels is due to inappropriate collagen-integrin interactions.

Methods

Derivation of iPS cells from AS patients

These studies have been carried out in accordance with the Declaration of Helsinki and approved by the Northern Health Human Research Ethics Committee. Fibroblasts from unrelated male patients with X-linked AS due to *COL4A5* missense mutations (p.G908R (AS1) or p.G624D (AS2)) were collected via biopsy. AS1 male mutation phenotype was severe, with early onset renal failure at age 14 years as well as hearing loss, lenticonus and central fleck retinopathy. AS2 male had renal failure onset at age 54 years, with hearing loss, no lenticonus but had central retinopathy (a much milder clinical phenotype). After skin biopsy, patient fibroblasts were cultivated in Dulbecco's Modified Eagle medium (DMEM, Invitrogen, Australia) with 10% fetal bovine serum (FBS; Invitrogen), 1% penicillin/streptomycin (Invitrogen) and 1% L-glutamine (Invitrogen) at 37 °C prior to reprogramming. Figure 1 panel (A) shows typical immunolabelling for fibroblast desmin. Skin biopsy derived dermal fibroblasts were plated in a 12 well plate (Falcon, USA) at a range of densities including 12,500, 25,000, 50,000 and 100,000 cells/well in duplicate. The plate was incubated for 2 days at 37^0C, 5% CO_2. At 80% confluence, one well was selected to reprogram based on viable appearance and cell density, the directions of CytoTuneTM-iPS 2.0 Sendai Reprogramming Kit (Thermo Fisher Scientific, USA) were applied to reprogram and resultant

cells were plated on a 1 million cell mouse embryonic fibroblast (MEF) feeder layer. Once colony formation was observed at 2-3 weeks post induction colonies were mechanically passaged using a 26 gauge needle onto new MEF layer. After reprogramming iPS cultures were maintained on a MEF feeder layer in ES media (DMEM/F12 media, GLUTAMAX, Knockout Serum Replacement, Non-essential Amino Acid (Gibco, USA) and 10ng/μl basic fibroblast growth factor (Merck Millipore, USA). Media was changed once daily for optimal cell growth/survival (Figure 1 panel (B) shows colonies expressing alkaline phosphatase activity). At this stage the colonies displayed a normal karyotype (Figure 1, panel C).

Differentiation of iPS cells to podocyte progenitors

iPS colonies were cut into small pieces and the cells transferred into MEF-coated organ culture dishes for 7 days prior to characterization studies. To initiate differentiation, iPS cell colonies were mechanically cut into pieces and cultured in geltrex (Life Technologies, Australia)-coated plates containing DMEM/F12 (Sigma-Aldrich, Australia) supplemented with 2.5% FBS, 1% NEAA, 100 μM β-mercaptoethanol, with 10 ng/ml activin A, 15 ng/ml BMP7 and 0.1 μM retinoic acid (all. Life Technologies). Figure 1, panel D, shows an overview of the podocyte differentiation protocol. To assess differentiation capacity, undifferentiated iPS cells were transplanted under the kidney capsule of immune-incompetent mice for 3 months where they formed cyst like structures (Figure 1, panel E). Within the cyst-like structures H&E staining showed the formation of crude glomerulus-like structures (Figure 1, panels F and G). For differentiation, cells were re-plated at day four and permitted a further six days of directed differentiation, the iPS-derived podocytes were grown for a further 10 days in DMEM/F12 without the activin A, BMP7 and retinoic acid, and were able to maintain their morphology and functional characteristics(Song et al., 2012). By day 10, colonies demonstrated a characteristic “cobblestone” morphology (Figure 1, panel H). By

day 20 podocyte-like cells exhibit the characteristic morphology of 2D cultured podocytes, ie large cells with intracytoplasmic extensions (Kabgani et al., 2012). Our previous studies have shown that this differentiation protocol markedly increases transcript and or protein levels for podocin, synaptopodin, WT-1, Pax2 and WT1 and nephrin at comparable levels to primary human podocytes (Song et al., 2012). Furthermore podocytes differentiated using this protocol were able to successfully integrate into developing kidney (Song et al., 2012). The key aspect of this previous work is that immunolabelling showed that large cells with intracytoplasmic extensions were immunoreactive for podocin, synaptopodin and WT-1; see figure 2 and figure 9 as exemplars of the morphologically distinct cell types that we select for imaging studies. Within the limitations of immunolabelling studies we report no observable differences in podocyte-specific immunolabelling between AS1, AS2 and NHMC podocytes (not shown). At no stage did we see evidence that any of these differentiated podocyte-like cells were immunoreactive for the fibroblast marker desmin.

For functional studies, podocyte-like cells were seeded onto either 6 well plates for qPCR or onto glass bottomed 35 mm dishes (MatTek®, USA) for calcium imaging and used at days 20-25 of differentiation (Figure 1, panel I).

Cell culture of immortalized podocytes

Human, SV40-T transformed podocytes (Saleem et al., 2002) (HIPs) were routinely cultured at 33^{o}C in RPMI 1640 medium with penicillin/streptomycin, insulin, transferrin, selenite and 10% fetal calf serum. Following splitting, these cells were incubated in the presence of 2% fetal calf serum at 37 ^{o}C for two weeks to reduce proliferation and promote differentiation prior to use.

Calcium Imaging

Calcium imaging studies were undertaken using a modification of a previously published protocol (Watmuff et al., 2015). Briefly, podocyte-like cells were loaded with FURA-2AM or Fluo4-AM (10μM, Molecular Probes, USA) for 30 min at 37°C. All experiments were performed in buffer (of composition, in mM, NaCl 145; $MgSO_4$ 1; KCl 5; glucose 10; HEPES 10) containing 0.1% BSA (w/v), pH 7.4. Depending upon the experimental protocol, the buffer contained 0, 0.2 or 2 mM or 0, 0.02, 0.2, 2 and 20 mM calcium chloride. A heated stage kept cells at 37°C while they were viewed with a Nikon Eclipse TE2000E microscope (Nikon, Japan) at 10× magnification. Within each field of view, 5−10 podocyte-like cells were chosen and analysis regions drawn within each cell.

For FURA-2 imaging, cells were illuminated alternately with 340/26 and 387/11nm light for 500ms in a 1.5s cycle. Emission was captured at 520/20 nm using a SPOT-RT camera (Diagnostic Instruments, USA) controlled by MetaFluor imaging software (v6.lr5, Universal Imaging Company, USA). Background emission values from excitation wavelengths (measured in a cell-free region) were subtracted from each image. The resultant emission values were expressed as an emission ratio (340:380 nm). All podocyte-like cells were allowed a 15-20 minute equilibration period prior to agonist addition.

Cumulative concentration-response curves and vehicle (buffer) responses were generated by the addition of calcium ($CaCl_2$, 0.2-20 mM in calcium free buffer) or angiotensin II (0.3-300nM in 2 mM $CaCl_2$ buffer). For gadolinium and spermidine cumulative concentration-response curves, podocyte-like cells were incubated in buffer containing 0.2 mM calcium throughout experimentation. Concentrations of vehicle (either buffer or 0.01% final concentration DMSO) were added to culture wells for 1-3 minutes before the addition of ligand. In some experiments, iberiotoxin (100nM (Cook et al., 2002)), tetraethylammonium (TEA, 5 mM(Lang et al., 2004)),

JPET Fast Forward. Published on August 13, 2018 as DOI: 10.1124/jpet.118.250142
This article has not been copyedited and formatted. The final version may differ from this version.

the focal adhesion kinase (FAK) inhibitor (PF562271 10nM, approximately 7 times its IC_{50} for FAK and 0.7 times its IC50 for Pyk2(Roberts et al., 2008)), or vehicle (0.01% DMSO) were added to cultures 10-15 minutes prior to the addition of calcium chloride.

The KCNMA1 channel opener, NS1619(Olesen et al., 1994) (1-10μM), was added cumulatively at 10min intervals.

To calculate ligand-induced elevations of $[Ca^{2+}]_i$, peak responses were expressed as a fraction of the average (340:380) emission ratio over the 25s period prior to the first addition of ligand or vehicle. To calculate ligand-induced reductions in $[Ca^{2+}]_i$, the post-ligand minimum response was expressed as a fraction of the average (340:380) emission ratio over the 25s period **immediately before** each addition of ligand.

Cellular (nM) calcium was calculated according to the method described by (Preston and Haynes, 2003) using the equation: $[Ca^{2+}]_i = K_D\beta$ ($(R-R_{min})/(R_{max}-R)$) (Grynkiewicz et al., 1985). β is the emission ratio, $R_{min}/R_{max,}$ at 380 nm. The K_D value (285 nM) was taken from(Groden et al., 1991). The R_{min} value was obtained in the presence of both 4-Br-A23187 (20μM) and EGTA (10 mM). The R_{max} was obtained in the presence of 4-Br-A23187 (20μM) and Ca^{2+} (100 mM). Mean and 95 % confidence interval data was calculated using $\log_{10}$ resting cytosolic $[Ca^{2+}]_i$ from each cell.

For AS1 replating experiments, cells were loaded with fluo4-AM (10μM, 30 min) and placed onto the heated stage of a Nikon A1R confocal microscope and illuminated at 488nm every second. Following equilibration (5-10 minutes) calcium chloride (0, 0.02, 0.2, 2 or 20 mM) was added over a 20 minute period. Nikon software was used to calculate emission intensity (520/20nm) in regions within cells. For analysis, background fluorescence intensity was subtracted from each cellular region of interest. To calculate acute reductions in $[Ca^{2+}]_i$, the post-

JPET Fast Forward. Published on August 13, 2018 as DOI: 10.1124/jpet.118.250142
This article has not been copyedited and formatted. The final version may differ from this version.

ligand minimum response was expressed as a fraction of the average fluorescence over the 25s period **immediately before** each addition of ligand.

Immunolabelling

Cells were processed as described previously(Song et al., 2012). Briefly, cells were fixed with 4% paraformaldehyde, labelled with anti-podocin, anti-WT-1 or anti-KCNMA1 antibodies (Abcam Australia, 1μg/ml 24hr, 4°C) followed by Alexa Fluor 488 or Alexa Fluor 555 secondary antibodies (1:1000, Molecular Probes, USA) for two hours at room temperature. Cells were counterstained with DAPI (1:10,000; Life Technologies) or Alexa 567 conjugated phalloidin (1:1000; Molecular Probes) prior to visualization with a Nikon A1R microscope.

Quantitative PCR

Quantitative PCR was undertaken using a method previously described(Watmuff et al., 2015). Briefly, total RNA was extracted from 10^6 cells using the Bioline RNA Mini kit according to manufacturer's instructions. Samples were analyzed for RNA content using a Nanodrop ND-1000 (Thermo Scientific, USA) spectrophotometer. Reactions were performed in triplicate on samples aggregated from at least three independently differentiating wells using the Bioline Sensifast SYBR No-ROX One Step Kit according to the manufacturer's specifications. KCNMA1 forward primer CCTGGCCTCCTCCATGGT (melting temperature, 60°C), reverse primer TTCTGGGCCTCCTTCGTCT (59°C). Relative gene expression was expressed as the ratio between target gene Ct values to β-actin Ct values.

Replating AS podocyte-like cells onto decellularized plates that had contained NHMC podocyte-like cells:

Decellularized tissue scaffolds, where removal of living cells leaves behind a cellular matrix that can influence culture differentiation and/or cellular function are commonly used in stem cell

biology (for example see (Morissette Martin et al., 2018)). We tested the idea that replating AS podocytes onto tissue culture plates that had contained NHMC cells could restore potassium channel function. Thus, we took tissue culture plates containing confluent monolayers of NHMC or AS1 podocyte-like cells and decellularized using the method of(Baiguera et al., 2013): briefly, plates were frozen (-80°C) and thawed four times, incubated with Milli-Q water (72 h at room temperature), and then processed twice with 1.0% Triton X-100 (60 min), water (30 min), 4.0% deoxycholate (60 min), water (30 min). After the last washing step, plates were washed with PBS prior to addition of AS1 podocyte-like cells. To extract AS1 podocyte-like cells from culture plates were incubated with TrypLE Select (Thermo Fisher, Australia) prior to centrifugation (150x*g*). Cells were re-suspended in culture media and plated into tissue culture plates that had contained AS1 or NHMC podocyte-like cells. Five days later the cells were used for Fluo-4 calcium imaging (as described above).

Statistical analysis:

Unless otherwise stated, results from experiments are presented as mean ± standard error of the mean (SEM) of at least 3 biological replicate experiments. Statistical analysis was performed on raw data with one- or two-way analysis of variance (ANOVA) followed by post-hoc Dunnett's test to show ligand effects vs vehicle response. All analysis was performed using PRISM v6.00 (GraphPad Software, USA). In all cases, a p-value of less than 0.05 was considered significant. Graphs are shown with ligand effects expressed as a fraction of the response to the appropriate vehicle.

Results

iPS cell derived podocyte-like cells express podocyte markers:

Differentiation generated cultures containing around 30-50% cells with podocyte-like morphology, ie. large flat cells with irregular borders. To qualitatively confirm the success of the directed differentiation pluripotent stem cell-derived podocyte-like cells were immunolabelled with antibodies for the podocyte markers Wilm's tumor-1 (WT1) and podocin (Song et al., 2012). At day 20 of differentiation, iPS-derived podocyte-like cells immunolabelled for both WT-1 and podocin (Figure 2). This expression was consistent with that observed in HIPs (Figure 2).

Resting Ca^{2+}: Following loading with FURA-2AM, average resting calcium was found to be significantly higher in AS1 and AS2 than in NHMC podocyte-like cells; 92 (with 95% confidence intervals, 68,126) and 90 (75,108), vs 55 (44,69) nM, respectively (One-way ANOVA of $\log_{10}$ resting calcium, with post-hoc Tukey's test, n = 5-9 biological replicates using 44-63 individual cells). Podocyte-like cells were identified in culture by having a podocyte-like cell morphology (see methods). These cells were generally quiescent with occasional spontaneous calcium transients (not shown).

Responses to extracellular calcium: HIPs

In calcium-free HEPES buffer, extracellular calcium ($[Ca^{2+}]_o$), the orthosteric ligand for the calcium-sensing receptor, elicited concentration-dependent changes in intracellular calcium ($[Ca^{2+}]_i$). These changes were evident as an acute depression of $[Ca^{2+}]_i$ preceding an elevation; Figure 3 panel A shows a typical response to 2 mM $[Ca^{2+}]_o$. Compared to vehicle control, $[Ca^{2+}]_o$ elicited both significant decreases and increases in $[Ca^{2+}]_i$ ($P<0.05$, one-way ANOVA with post-hoc Dunnett's test, n = 31 cells from five replicate experiments; Figure 3, panels B and C). We then assessed effects on $[Ca^{2+}]_i$ of two other activators of the calcium sensing receptor, the polyamine, spermidine, and the trivalent cation, gadolinium (Gd^{3+}). Spermidine but not Gd^{3+}

JPET Fast Forward. Published on August 13, 2018 as DOI: 10.1124/jpet.118.250142
This article has not been copyedited and formatted. The final version may differ from this version.

elicited both concentration-dependent decreases and increases in $[Ca^{2+}]_i$, (Figure 3, panels B and C).

Given the relationship between calcium sensing receptors and large conductance calcium activated potassium (KCNMA1) channels(Vysotskaya et al., 2014), we explored the possibility that KCNMA1 channels might be responsible for the reductions in $[Ca^{2+}]_i$ that preceded elevations. We therefore incubated podocyte-like cells with the KCNMA1 channel inhibitor, iberiotoxin (100nM), as well as the less specific voltage gated potassium channel blocker, tetraethylammonium (TEA, 5 mM), prior to the addition of $[Ca^{2+}]_o$. Neither iberiotoxin, or TEA affected the maximal elevations or inhibitions of $[Ca^{2+}]_i$ in response to $[Ca^{2+}]_o$ (Figure 3, panels D and E).

Responses to extracellular calcium: NHMC podocyte-like cells

In calcium-free HEPES buffer, $[Ca^{2+}]_o$ also elicited changes in $[Ca^{2+}]_i$ in NHMC podocyte-like cells. These changes were evident in a rapid decrease followed by a rapid elevation of $[Ca^{2+}]_i$ (Figure 4, panel A shows a typical response to 2 mM $[Ca^{2+}]_o$; n = 72 cells from six replicate experiments). As with the HIPs, spermidine, but not Gd^{3+}, produced both elevations and inhibitions of $[Ca^{2+}]_i$ (Figure 4, panels B and C).

Both iberiotoxin (100 nM) and TEA (5 mM) had no effect on $[Ca^{2+}]_o$-induced elevations of $[Ca^{2+}]_i$ (Figure 4, panel D), but both ligands prevented the acute decreases in $[Ca^{2+}]_i$ (Figure 4, panel E) in response to $[Ca^{2+}]_o$, indicating that the acute reductions were due to KCNMA1 channel activity. These channels are known to be modulated by focal adhesion kinase(Rezzonico et al., 2003), so we incubated cells with the selective focal adhesion kinase inhibitor, PF562271 (10 nM), before the addition of $[Ca^{2+}]_o$. This kinase inhibitor increased responses to $[Ca^{2+}]_o$ and prevented acute

JPET Fast Forward. Published on August 13, 2018 as DOI: 10.1124/jpet.118.250142
This article has not been copyedited and formatted. The final version may differ from this version.

reductions in $[Ca^{2+}]_i$ (Figure 4, panels D and E) possibly indicating an interaction between focal adhesion kinase and KCNMA1 channels in NHMC podocyte-like cells.

Responses to extracellular calcium: AS1 podocyte-like cells

In contrast to both HIPs and NHMC podocyte-like cells, AS1 podocyte-like cells responded to $[Ca^{2+}]_o$ only with elevations of $[Ca^{2+}]_i$ (n = 33 cells from five replicate experiments). Figure 5, panel A shows a typical response to 2 mM $[Ca^{2+}]_o$. Spermidine, but not Gd^{3+}, was an effective elevator of $[Ca^{2+}]_i$ (Figure 5, panel B) but neither spermidine or $[Ca^{2+}]_o$ produced reductions in $[Ca^{2+}]_i$ (Figure 5, panel C). Neither tetraethylammonium (TEA, 5 mM), iberiotoxin (100 nM) nor PF562271 (10 nM) reduced the magnitude of elevations in $[Ca^{2+}]_i$ in AS1 podocyte-like cells ($P<0.01$, one way ANOVA with post-hoc Dunnett's, n = 33 values from five replicate experiments, Figure 5, panel D). Neither TEA, iberiotoxin nor PF562271 promoted the appearance of an acute reduction in intracellular calcium (Figure 5, panel E).

Responses to extracellular calcium: AS2 podocyte-like cells

The AS2 podocyte-like cell responses to $[Ca^{2+}]_o$ were similar to the AS1 cell line, with concentration-dependent elevations, but no acute decreases in $[Ca^{2+}]_i$ (Figure 6, panels A, B and C).

Large conductance calcium activated potassium channel activity

Given the role of KCNMA1 channels in podocyte function(Tao et al., 2016) and our own evidence of an effect, we further investigated the possibility that these channels were functional only in NHMC podocytes. The KCNMA1 channel opener, NS1619 (1 -10 μM), elicited concentration-dependent reductions in basal calcium in both NHMC and HIP, but not AS1 podocyte-like cells (Figure 7).

Responses to angiotensin II:

JPET Fast Forward. Published on August 13, 2018 as DOI: 10.1124/jpet.118.250142
This article has not been copyedited and formatted. The final version may differ from this version.

We next assessed whether another G-protein coupled receptor, the angiotensin II receptor, could elicit both elevations and inhibitions of $[Ca^{2+}]_i$. Although angiotensin II elicited robust elevations of intracellular calcium in NHMC, HIP and AS1 and weak responses in AS2 podocyte-like cells we rarely saw any evidence of concentration-dependence or acute decreases in intracellular calcium prior to elevations (not shown). However, responses to angiotensin II (0.3-300nM) were robustly blocked by the AT1 receptor antagonist, losartan (1μM), but not by the AT2 receptor antagonist PD123,319 (1μM) in all groups tested (Figure 8).

qPCR and immunolabelling. Since our data indicated the absence of functional KCNMA1 channels in AS patient derived podocyte-like cells, we undertook qPCR and immunolabelling studies to identify whether transcript and protein for this receptor were present. We found largely equivalent levels of KCNMA1 transcript in AS1, but significantly reduced transcript ($P<0.05$, one way ANOVA with post-hoc Dunnett's test) present in immortalized podocyte-like cells (expressed as a fraction of NHMC podocyte-like cells values: 1.29 ± 0.34 (3) for AS1 and 0.18 ± 0.13 (2) for HIP, (N) values). Nonetheless, immunolabelling showed evidence of KCNMA1 protein in all three cell lines tested (Figure 9 shows typical labelling). We then tested the theory that replating AS1 podocyte-like cells onto decellularized plates of NHMC podocyte-like cells could restore channel function.

Effects of replating AS podocyte-like cells onto decellularized plates that had contained NHMC podocyte-like cells:

Following decellularization, plates were devoid of any sign of cells or cellular debris (not shown). AS1 podocyte-like cells cultivated upon plates that once contained NHMC podocyte-like cells responded to lower concentrations of extracellular calcium with acute reductions of $[Ca^{2+}]_i$ that

JPET Fast Forward. Published on August 13, 2018 as DOI: 10.1124/jpet.118.250142
This article has not been copyedited and formatted. The final version may differ from this version.

were not evident in AS1 podocytes re-plated onto decellularized AS1 podocyte plates ($P<0.001$, two way-ANONA with post-hoc Dunnett's test, Figure 10). The acute reductions in intracellular calcium could be inhibited be TEA (5mM, Figure 10).

Discussion

In this study we compare the activities of podocyte-like cells derived from AS patients, a healthy individual and a commonly utilized, immortalized podocyte cell line. Consistent with our previous work(Song et al., 2011; Song et al., 2012), the iPS cells used for this study showed expression of markers commonly used to identify podocytes; WT-1 and podocin. We then investigated whether AS patient-derived podocyte-like cells showed any discernible functional phenotype associated with the regulation of intracellular calcium; a critical regulator of function and survival in many cell types(van Empel and De Windt, 2004; Mattson, 2007; Oh et al., 2011). Podocyte-like cells were largely quiescent with infrequent spontaneous elevations of intracellular calcium. Resting $[Ca^{2+}]_i$ in both AS1 and AS2 podocyte-like cells (~90nM) was significantly greater than in NHMC podocyte-like cells (~55nM). However, these values lie within previously reported values in human primary 113±22(Foster et al., 2003) as well as human immortalized; 146$\pm$76(Ardaillou et al., 1996), 102±35(Foster et al., 2003), and mouse immortalized podocyte-like cells 49$\pm$11(Huber et al., 1998), 82$\pm$12(Fischer et al., 2002). The variability of these data may be attributable to different assay methods and or the presence of the spontaneous calcium fluctuations. That our assay shows significantly higher $[Ca^{2+}]_i$ in the AS podocyte-like cells may indicate some difference in calcium handling capability.

We next determined whether the podocyte-like cell cultures showed differences in response to two G-protein coupled receptors that have profound effects on podocyte function and survival; the CaSR and angiotensin II receptors. The CaSR belongs to the family C G-protein coupled receptors,

JPET Fast Forward. Published on August 13, 2018 as DOI: 10.1124/jpet.118.250142
This article has not been copyedited and formatted. The final version may differ from this version.

it is expressed throughout the body, especially the thyroid and parathyroid glands, kidney, bone and brain(Brown, 1991; Brown and Macleod, 2001). Although widely distributed within the kidney(Riccardi and Brown, 2010), it is highly localized at the endoplasmic reticulum and the cell plasma membrane especially at, or close to podocyte slit diaphragms(Oh et al., 2011). This receptor plays a pivotal role in podocyte survival in sub-total nephrectomized rats(Ogata et al., 2003) and more recently Oh and co-workers suggested that positive allosteric modulators (activators) of the CaSR limit antibiotic-induced podocyte damage via phosphorylated-ERK mediated anti-apoptotic and cytoskeleton-stabilizing effects(Oh et al., 2011).

In response to the orthosteric activator of the CaSR, extracellular calcium, all podocyte-like cells showed elevations of $[Ca^{2+}]_i$. We then tested two other ligands known to activate the calcium sensing receptor, gadolium(Brown et al., 1993) and spermidine(Quinn et al., 1997). Gadolinium was ineffective across all cell lines tested, however, this lack of effect should be viewed with caution since Gd^{3+} has been shown to suppress receptor-activated TRP and ORAI (calcium release-activated calcium channel protein 1(Malasics et al., 2010; Bouron et al., 2015; Xu et al., 2015)) activity. In contrast, the polyamine, spermidine was as effective modulator of $[Ca^{2+}]_i$. Prior to elevations of intracellular calcium, we noted that both spermidine and $[Ca^{2+}]_o$ elicited a transient decrease in $[Ca^{2+}]_i$ in HIPs and NHMC, but not AS podocyte–like cells. One of the most striking aspects of responses to spermidine in the four cell "lines" was the inconsistency of response. While the morphology of the podocyte-like cells was consistent, particularly across the induced pluripotent stem cell derived lines, the responses to extracellular calcium and spermidine were not. Thus while extracellular calcium robustly increased intracellular calcium in NHMC podocyte-like cells, responses in HIP, AS1 and AS2 were greatly reduced. More curious perhaps was the observation that responses to spermidine were relatively consistent in AS1 and NHMC. Whether

this effect relates to differences in calcium sensing receptor mutations, function or expression, or more generic differences in cell lines is currently unknown. Consistent with this inconsistency, modulators of potassium channels produced little change in extracellular calcium induced elevations of intracellular calcium in HIP and NHMC, while TEA appeared to produce a truncated response in AS1 podocyte-like cells. Similarly, focal adhesion kinase inhibition produced a marked increase in extracellular calcium-induced maximal response in NHMC podocyte-like cells, but a profound decrease in AS1 podocyte like cells. At present we believe that these disparate effects may result from differing states of tonic channel or kinase activity within each cell line. Perhaps of more significance is the idea that our observations raise questions about the suitability of single cell lines as exemplars of cell function. While much is made of isogenic control modifications for induced pluripotent stem cell derived cells, our observations indicate that caution must be observed in conclusions based upon single cell-line experiments since any one of these cell lines may not be representative of broader aspects of "typical" physiological behavior.

Since elevations of intracellular calcium can activate KCNMA1 channels(Tao et al., 2016), we assessed whether blockers of this channel, iberiotoxin and TEA(Singh et al., 2012), could inhibit transient decreases in $[Ca^{2+}]_i$. In NHMC podocyte-like cells, but not HIPs, the reductions of intracellular calcium were blocked by both iberiotoxin and TEA. The insensitivity of the immortalized podocyte-like cells to KCNMA1 blockers may indicate that this channel was either not present or functional, or that other calcium activated potassium channels were capable of masking its activity. In a second effort to establish whether this channel was present we assessed effects of the KCNMA1 channel opener, NS1619(Debska et al., 2003). NHMC and HIP, but not AS1 podocyte-like cells showed decreases in intracellular calcium in response to NS1619,

indicating the presence of KCNMA1 channels. To confirm the presence of these channels we assessed AS1, NHMC and HIP cultures for KCNMA1 channel mRNA. Surprisingly, we found this transcript to be universally expressed, with little difference in expression in AS1 and NHMC cultures. This finding indicates that while the channel transcript is present in AS podocyte-like cells, the protein may not be. To ascertain whether the channel protein was present we used immunolabelling and found the channel present in all cell lines; particularly in regions around the periphery of AS1 and NHMC podocyte-like cells. Given the presence of transcript and immunolabelled protein, we conclude that AS1 podocyte-like cells possess KCNMA1 channels, but they are not functional. The absence of functional KCNMA1 channels may have ramifications for podocyte survival since KCNMA1 channels are significant regulators of activity in podocytes and other cell types. In podocytes, KCNMA1 channels localize with nephrin and may regulate podocyte activity in response to stretching (Morton et al., 2004), although more complex interactions involving synaptopodin, Rho and cytoskeletal proteins are also likely (Kim et al., 2010). In other cell types, KCNMA1 activation can protect cardiomyoblast cells from hypoxia/reperfusion damage(Fretwell and Dickenson, 2011) and reduce shock-induced reductions in vascular reactivity(Hu et al., 2014). KCNMA1 channel activity can also facilitate prostate cancer cell growth possibly through an association with αvβ3 integrin and focal adhesion kinase(Du et al., 2016). Although the absence of potassium channel function may explain the elevated intracellular calcium in AS1 (and AS2) podocyte-like cells, the mechanism underlying this effect was not immediately clear. Interestingly in HIPs iberiotoxin and TEA did not block the acute reductions in $[Ca^{2+}]_i$, but NS1619 showed an effect and qPCR indicated the presence, albeit at relatively low levels, of KCNMA1 transcript. At present we speculate that KCNMA1 channels are present on these cells, but may be present with additional TEA and iberiotoxin-insensitive

small conductance calcium activated potassium channels(Sah, 1996). Whether this makes these cells a better or worse *in vitro* model of podocyte function than pluripotent stem cell derived podocyte-like cells is unclear.

There is evidence linking the integrin linked focal adhesion kinase(So et al., 2011), the related kinase Pyk2(Ling et al., 2004) as well as src(Yang et al., 2010), with the modulation of KCNMA1 channel activity in other cell types, so we speculated that collagen gene mutations in AS podocyte-like cells impacted upon integrin signalling. To investigate this idea we assessed the influence of the selective focal adhesion kinase inhibitor PF562271 upon transient decreases in $[Ca^{2+}]_i$ and found it to abolish the acute reduction in intracellular calcium in NHMC podocyte-like cells. Although this data indicates some form of relationship between integrin signalling, focal adhesion kinase and potassium channel signalling in podocytes, much more work is needed to identify the specific mechanisms underlying interaction.

We investigated whether another G-protein coupled receptor known to modulate podocyte activity, the angiotensin II receptor (Nitschke et al., 2000; Hsu et al., 2008; Ilatovskaya et al., 2014), also showed acute decreases in intracellular calcium prior to elevations. Consistent with the idea that angiotensin II interacts with TRPC6 channels to elevate intracellular calcium (Ilatovskaya *et al.*, 2014), angiotensin II elevated, without acute decreases, intracellular calcium at all concentrations tested. That these responses were predominantly blocked by the Angiotensin II receptor antagonist, losartan, indicates a major role of the angiotensin II type 1 receptor in regulating acute elevations of intracellular calcium, a finding consistent with that reported in rat podocytes (Henger et al., 1997). As calcium, but not angiotensin II promoted acute reductions in intracellular calcium we believe that this may indicate specific coupling of G-protein coupled receptors to potassium channels in podocytes.

JPET Fast Forward. Published on August 13, 2018 as DOI: 10.1124/jpet.118.250142
This article has not been copyedited and formatted. The final version may differ from this version.

The extracellular matrix plays a significant role in regulating cell and tissue function and many studies have employed decellularized tissue matrices to regulate the growth and survival of a number of different cell types, from hepatocytes (Lorvellec et al., 2017) to cardiomyocytes (Eitan et al., 2010). A smaller body of literature also indicates that 2D cultures can generate their own matrix which, after decellularization can be applied to new culture vessels (Decaris et al., 2012) or used as a substrate for re-seeding (Pham et al., 2008). Since our PCR evidence indicated that KCNMA1 channels were present, but not functional, in AS1 podocyte-like cells, we tested the idea that re-plating AS podocyte-like cells onto surfaces once occupied by NHMC cells could help restore channel activity. Following plating upon decellularized NHMC plates we observed a small, but significant reduction in $[Ca^{2+}]_i$ in AS1 podocyte-like cells following the addition of extracellular calcium. This effect was not evident in AS1 cells seeded onto decellularized AS1 plates. That this effect was also blocked by TEA indicated an effect through potassium channels. Given the findings that (i) inhibition of FAK blocked the transient reduction in intracellular calcium in response to extracellular calcium and, (ii) replating of AS1 podocyte-like cells upon NHMC decellularized plates, promoted a TEA-sensitive reduction of intracellular calcium, we suggest that the KCNMA1 channels require appropriate integrin-FAK signalling for function. While we show that calcium sensing receptor activating ligands produce fundamentally different effects in immortalized, non-AS and AS patient derived podocyte-like cells, possibly through changes in KCNMA1 channel function, we must acknowledge the limitations of the current approach. The first of those limitations is that we show differences in some aspects of podocyte-like cell function using data from a limited sample size; two patient-derived, one control-derived and one immortalized cell line. The second potential limitation is that, while our podocyte-like cells possess the morphological and immunocytochemical profile of podocytes, *in vitro* studies

may not truly show the functional properties of podocytes *in situ*. In spite of these limitations our studies demonstrate that induced pluripotent stem cell derived podocyte-like cells may represent a useful system for basic mechanistic and pharmacological studies of heritable kidney disease.

Acknowledgements

Authorship contributions

Participated in research design: Haynes

Conducted experiments: Haynes, Lieuw, Selby, Abad, Saini, Fisher, Ho and Vandekolk

Contributed new reagents or analytic tools: Savige

Performed data analysis: Haynes

Wrote or contributed to the writing of the manuscript: Haynes, Ricardo and Leach

References

Ardaillou N, Blaise V, Costenbader K, Vassitch Y and Ardaillou R (1996) Characterization of a B2-bradykinin receptor in human glomerular podocytes. *The American journal of physiology* **271**:F754-761.

Baiguera S, Del Gaudio C, Lucatelli E, Kuevda E, Boieri M, Mazzanti B, Bianco A and Macchiarini P (2013) Electrospun gelatin scaffolds incorporating rat decellularized brain extracellular matrix for neural tissue engineering. *Biomaterials*.

Barker DF, Hostikka SL, Zhou J, Chow LT, Oliphant AR, Gerken SC, Gregory MC, Skolnick MH, Atkin CL and Tryggvason K (1990) Identification of mutations in the COL4A5 collagen gene in Alport syndrome. *Science* **248**:1224-1227.

Blattner SM and Kretzler M (2005) Integrin-linked kinase in renal disease: connecting cell-matrix interaction to the cytoskeleton. *Current opinion in nephrology and hypertension* **14**:404-410.

Bouron A, Kiselyov K and Oberwinkler J (2015) Permeation, regulation and control of expression of TRP channels by trace metal ions. *Pflugers Archiv : European journal of physiology* **467**:1143-1164.

Brown EM (1991) Extracellular Ca^{2+} sensing, regulation of parathyroid cell function, and role of Ca^{2+} and other ions as extracellular (first) messengers. *Physiol Rev* **71**:371-411.

Brown EM, Gamba G, Riccardi D, Lombardi M, Butters R, Kifor O, Sun A, Hediger MA, Lytton J and Hebert SC (1993) Cloning and characterization of an extracellular Ca(2+)-sensing receptor from bovine parathyroid. *Nature* **366**:575-580.

Brown EM and Macleod RJ (2001) Extracellular calcium sensing and extracellular calcium signaling. *Physiol Rev* **81**:239-297.

Cook AL, Frydenberg M and Haynes JM (2002) Protein kinase G activation of K(ATP) channels in human-cultured prostatic stromal cells. *Cellular signalling* **14**:1023-1029.

Cosgrove D (2011) Glomerular pathology in Alport syndrome: a molecular perspective. *Pediatric nephrology*.

Debska G, Kicinska A, Dobrucki J, Dworakowska B, Nurowska E, Skalska J, Dolowy K and Szewczyk A (2003) Large-conductance K+ channel openers NS1619 and NS004 as inhibitors of mitochondrial function in glioma cells. *Biochem Pharmacol* **65**:1827-1834.

Decaris ML, Mojadedi A, Bhat A and Leach JK (2012) Transferable cell-secreted extracellular matrices enhance osteogenic differentiation. *Acta biomaterialia* **8**:744-752.

Du C, Zheng Z, Li D, Chen L, Li N, Yi X, Yang Y, Guo F, Liu W, Xie X and Xie M (2016) BKCa promotes growth and metastasis of prostate cancer through facilitating the coupling between alphavbeta3 integrin and FAK. *Oncotarget* **7**:40174-40188.

Eitan Y, Sarig U, Dahan N and Machluf M (2010) Acellular cardiac extracellular matrix as a scaffold for tissue engineering: in vitro cell support, remodeling, and biocompatibility. *Tissue engineering Part C, Methods* **16**:671-683.

Feingold J, Bois E, Chompret A, Broyer M, Gubler MC and Grunfeld JP (1985) Genetic heterogeneity of Alport syndrome. *Kidney Int* **27**:672-677.

Fischer KG, Huber TB, Henger A, Fink E, Schwertfeger E, Rump LC and Pavenstadt H (2002) Eluate derived by extracorporal antibody-based immunoadsorption elevates the cytosolic Ca2+ concentration in podocytes via B2 kinin receptors. *Kidney & blood pressure research* **25**:384-393.

Foster RR, Hole R, Anderson K, Satchell SC, Coward RJ, Mathieson PW, Gillatt DA, Saleem MA, Bates DO and Harper SJ (2003) Functional evidence that vascular endothelial growth factor may act as an autocrine factor on human podocytes. *American journal of physiology Renal physiology* **284**:F1263-1273.

Fretwell L and Dickenson JM (2011) Role of large-conductance Ca(2)+-activated K+ channels in adenosine A(1) receptor-mediated pharmacological postconditioning in H9c2 cells. *Canadian journal of physiology and pharmacology* **89**:24-30.

Greka A and Mundel P (2012) Cell biology and pathology of podocytes. *Annu Rev Physiol* **74**:299-323.

Groden DL, Guan Z and Stokes BT (1991) Determination of Fura-2 dissociation constants following adjustment of the apparent Ca-EGTA association constant for temperature and ionic strength. *Cell calcium* **12**:279-287.

Grynkiewicz G, Poenie M and Tsien RY (1985) A new generation of Ca2+ indicators with greatly improved fluorescence properties. *The Journal of biological chemistry* **260**:3440-3450.

Henger A, Huber T, Fischer KG, Nitschke R, Mundel P, Schollmeyer P, Greger R and Pavenstadt H (1997) Angiotensin II increases the cytosolic calcium activity in rat podocytes in culture. *Kidney Int* **52**:687-693.

Hsu HH, Hoffmann S, Endlich N, Velic A, Schwab A, Weide T, Schlatter E and Pavenstadt H (2008) Mechanisms of angiotensin II signaling on cytoskeleton of podocytes. *Journal of molecular medicine* **86**:1379-1394.

Hu Y, Yang G, Xiao X, Liu L and Li T (2014) Bkca opener, NS1619 pretreatment protects against shock-induced vascular hyporeactivity through PDZ-Rho GEF-RhoA-Rho kinase pathway in rats. *The journal of trauma and acute care surgery* **76**:394-401.

Huber TB, Gloy J, Henger A, Schollmeyer P, Greger R, Mundel P and Pavenstadt H (1998) Catecholamines modulate podocyte function. *Journal of the American Society of Nephrology : JASN* **9**:335-345.

Hudson BG, Tryggvason K, Sundaramoorthy M and Neilson EG (2003) Alport's syndrome, Goodpasture's syndrome, and type IV collagen. *N Engl J Med* **348**:2543-2556.

Ilatovskaya DV, Palygin O, Chubinskiy-Nadezhdin V, Negulyaev YA, Ma R, Birnbaumer L and Staruschenko A (2014) Angiotensin II has acute effects on TRPC6 channels in podocytes of freshly isolated glomeruli. *Kidney Int* **86**:506-514.

Ishida Y and Nagata K (2011) Hsp47 as a collagen-specific molecular chaperone. *Methods Enzymol* **499**:167-182.

Kabgani N, Grigoleit T, Schulte K, Sechi A, Sauer-Lehnen S, Tag C, Boor P, Kuppe C, Warsow G, Schordan S, Mostertz J, Chilukoti RK, Homuth G, Endlich N, Tacke F, Weiskirchen R, Fuellen G, Endlich K, Floege J, Smeets B and Moeller MJ (2012) Primary cultures of glomerular parietal epithelial cells or podocytes with proven origin. *PloS one* **7**:e34907.

Kim EY, Suh JM, Chiu YH and Dryer SE (2010) Regulation of podocyte BK(Ca) channels by synaptopodin, Rho, and actin microfilaments. *American journal of physiology Renal physiology* **299**:F594-604.

Lang RJ, Haynes JM, Kelly J, Johnson J, Greenhalgh J, O'Brien C, Mulholland EM, Baker L, Munsie M and Pouton CW (2004) Electrical and neurotransmitter activity of mature neurons derived from mouse embryonic stem cells by Sox-1 lineage selection and directed differentiation. *The European journal of neuroscience* **20**:3209-3221.

Liebau MC, Lang D, Bohm J, Endlich N, Bek MJ, Witherden I, Mathieson PW, Saleem MA, Pavenstadt H and Fischer KG (2006) Functional expression of the renin-angiotensin system in human podocytes. *American journal of physiology Renal physiology* **290**:F710-719.

Ling S, Sheng JZ and Braun AP (2004) The calcium-dependent activity of large-conductance, calcium-activated K+ channels is enhanced by Pyk2- and Hck-induced tyrosine phosphorylation. *American journal of physiology Cell physiology* **287**:C698-706.

Lorvellec M, Scottoni F, Crowley C, Fiadeiro R, Maghsoudlou P, Pellegata AF, Mazzacuva F, Gjinovci A, Lyne AM, Zulini J, Little D, Mosaku O, Kelly D, De Coppi P and Gissen P (2017) Mouse decellularised liver scaffold improves human embryonic and induced pluripotent stem cells differentiation into hepatocyte-like cells. *PloS one* **12**:e0189586.

Malasics A, Boda D, Valisko M, Henderson D and Gillespie D (2010) Simulations of calcium channel block by trivalent cations: Gd(3+) competes with permeant ions for the selectivity filter. *Biochimica et biophysica acta* **1798**:2013-2021.

Mattson MP (2007) Calcium and neurodegeneration. *Aging Cell* **6**:337-350.

Mochizuki T, Lemmink HH, Mariyama M, Antignac C, Gubler MC, Pirson Y, Verellen-Dumoulin C, Chan B, Schroder CH, Smeets HJ and et al. (1994) Identification of mutations in the alpha 3(IV) and alpha 4(IV) collagen genes in autosomal recessive Alport syndrome. *Nat Genet* **8**:77-81.

Morissette Martin P, Shridhar A, Yu C, Brown C and Flynn LE (2018) Decellularized Adipose Tissue Scaffolds for Soft Tissue Regeneration and Adipose-Derived Stem/Stromal Cell Delivery. *Methods in molecular biology* **1773**:53-71.

Morton MJ, Hutchinson K, Mathieson PW, Witherden IR, Saleem MA and Hunter M (2004) Human podocytes possess a stretch-sensitive, Ca2+-activated K+ channel: potential implications for the control of glomerular filtration. *Journal of the American Society of Nephrology : JASN* **15**:2981-2987.

Mundel P and Kriz W (1995) Structure and function of podocytes: an update. *Anat Embryol (Berl)* **192**:385-397.

Nitschke R, Henger A, Ricken S, Gloy J, Muller V, Greger R and Pavenstadt H (2000) Angiotensin II increases the intracellular calcium activity in podocytes of the intact glomerulus. *Kidney Int* **57**:41-49.

Obeidova H, Merta M, Reiterova J, Maixnerova D, Stekrova J, Rysava R and Tesar V (2006) Genetic basis of nephrotic syndrome--review. *Prague Med Rep* **107**:5-16.

Ogata H, Ritz E, Odoni G, Amann K and Orth SR (2003) Beneficial effects of calcimimetics on progression of renal failure and cardiovascular risk factors. *Journal of the American Society of Nephrology : JASN* **14**:959-967.

Oh J, Beckmann J, Bloch J, Hettgen V, Mueller J, Li L, Hoemme M, Gross ML, Penzel R, Mundel P, Schaefer F and Schmitt CP (2011) Stimulation of the calcium-sensing receptor stabilizes the podocyte cytoskeleton, improves cell survival, and reduces toxin-induced glomerulosclerosis. *Kidney Int* **80**:483-492.

Olesen SP, Munch E, Moldt P and Drejer J (1994) Selective activation of Ca(2+)-dependent K+ channels by novel benzimidazolone. *European journal of pharmacology* **251**:53-59.

Pham QP, Kasper FK, Scott Baggett L, Raphael RM, Jansen JA and Mikos AG (2008) The influence of an in vitro generated bone-like extracellular matrix on osteoblastic gene expression of marrow stromal cells. *Biomaterials* **29**:2729-2739.

Pieri M, Stefanou C, Zaravinos A, Erguler K, Stylianou K, Lapathitis G, Karaiskos C, Savva I, Paraskeva R, Dweep H, Sticht C, Anastasiadou N, Zouvani I, Goumenos D, Felekkis K,

Saleem M, Voskarides K, Gretz N and Deltas C (2014) Evidence for Activation of the Unfolded Protein Response in Collagen IV Nephropathies. *Journal of the American Society of Nephrology : JASN* **25**:260-275.

Preston A and Haynes JM (2003) alpha(1)-Adrenoceptor effects mediated by protein kinase C alpha in human cultured prostatic stromal cells. *Br J Pharmacol* **138**:218-224.

Quinn SJ, Ye CP, Diaz R, Kifor O, Bai M, Vassilev P and Brown E (1997) The Ca2+-sensing receptor: a target for polyamines. *The American journal of physiology* **273**:C1315-1323.

Reiser J, Kriz W, Kretzler M and Mundel P (2000) The glomerular slit diaphragm is a modified adherens junction. *Journal of the American Society of Nephrology : JASN* **11**:1-8.

Rezzonico R, Cayatte C, Bourget-Ponzio I, Romey G, Belhacene N, Loubat A, Rocchi S, Van Obberghen E, Girault JA, Rossi B and Schmid-Antomarchi H (2003) Focal adhesion kinase pp125FAK interacts with the large conductance calcium-activated hSlo potassium channel in human osteoblasts: potential role in mechanotransduction. *J Bone Miner Res* **18**:1863-1871.

Riccardi D and Brown EM (2010) Physiology and pathophysiology of the calcium-sensing receptor in the kidney. *American journal of physiology Renal physiology* **298**:F485-499.

Roberts WG, Ung E, Whalen P, Cooper B, Hulford C, Autry C, Richter D, Emerson E, Lin J, Kath J, Coleman K, Yao L, Martinez-Alsina L, Lorenzen M, Berliner M, Luzzio M, Patel N, Schmitt E, LaGreca S, Jani J, Wessel M, Marr E, Griffor M and Vajdos F (2008) Antitumor activity and pharmacology of a selective focal adhesion kinase inhibitor, PF-562,271. *Cancer research* **68**:1935-1944.

Sah P (1996) Ca(2+)-activated K+ currents in neurones: types, physiological roles and modulation. *Trends in neurosciences* **19**:150-154.

Saleem MA, O'Hare MJ, Reiser J, Coward RJ, Inward CD, Farren T, Xing CY, Ni L, Mathieson PW and Mundel P (2002) A conditionally immortalized human podocyte cell line demonstrating nephrin and podocin expression. *Journal of the American Society of Nephrology : JASN* **13**:630-638.

Shankland SJ, Pippin JW, Reiser J and Mundel P (2007) Podocytes in culture: past, present, and future. *Kidney Int* **72**:26-36.

Singh SK, O'Hara B, Talukder JR and Rajendran VM (2012) Aldosterone induces active K(+) secretion by enhancing mucosal expression of Kcnn4c and Kcnma1 channels in rat distal colon. *American journal of physiology Cell physiology* **302**:C1353-1360.

So EC, Wu KC, Liang CH, Chen JY and Wu SN (2011) Evidence for activation of BK Ca channels by a known inhibitor of focal adhesion kinase, PF573228. *Life Sci* **89**:691-701.

Song B, Niclis JC, Alikhan MA, Sakkal S, Sylvain A, Kerr PG, Laslett AL, Bernard CA and Ricardo SD (2011) Generation of induced pluripotent stem cells from human kidney mesangial cells. *Journal of the American Society of Nephrology : JASN* **22**:1213-1220.

Song B, Smink AM, Jones CV, Callaghan JM, Firth SD, Bernard CA, Laslett AL, Kerr PG and Ricardo SD (2012) The directed differentiation of human iPS cells into kidney podocytes. *PloS one* **7**:e46453.

Tao J, Lan Z, Wang Y, Hei H, Tian L, Pan W, Zhang X and Peng W (2016) Large-Conductance Calcium-Activated Potassium Channels in Glomerulus: From Cell Signal Integration to Disease. *Front Physiol* **7**:248.

van Empel VP and De Windt LJ (2004) Myocyte hypertrophy and apoptosis: a balancing act. *Cardiovasc Res* **63**:487-499.

Vysotskaya ZV, Moss CR, 2nd, Gilbert CA, Gabriel SA and Gu Q (2014) Modulation of BK channel activities by calcium-sensing receptor in rat bronchopulmonary sensory neurons. *Respiratory physiology & neurobiology* **203**:35-44.

Watmuff B, Hartley BJ, Hunt CP, Fabb SA, Pouton CW and Haynes JM (2015) Human pluripotent stem cell derived midbrain PITX3(eGFP/w) neurons: a versatile tool for pharmacological screening and neurodegenerative modeling. *Frontiers in cellular neuroscience* **9**:1-15.

Xu YJ, Elimban V and Dhalla NS (2015) Reduction of blood pressure by store-operated calcium channel blockers. *Journal of cellular and molecular medicine* **19**:2763-2770.

Yang Y, Wu X, Gui P, Wu J, Sheng JZ, Ling S, Braun AP, Davis GE and Davis MJ (2010) Alpha5beta1 integrin engagement increases large conductance, Ca2+-activated K+ channel current and Ca2+ sensitivity through c-src-mediated channel phosphorylation. *The Journal of biological chemistry* **285**:131-141.

Footnotes

This work was supported by the Alport Foundation of Australia and the Kidney Foundation of Canada.

Legends for Figures

Figure 1. Induced pluripotent stem cell-derived podocyte-like cells. Panel (A) shows dermal fibroblasts from AS patient, prior to reprogramming, immunolabelled for desmin (green) and DAPI (blue). Panel (B) shows a low power image of a colony expressing alkaline phosphatase activity and expressing a normal karyotype (panel C). Panel (D) provides an overview of the differentiation method for pluripotent stem cell derived podocyte-like cell differentiation. At day four of differentiation cells were re-plated or transplanted under the kidney capsule of immune-competent mice where they formed cyst like structures at day 20 (Figure 1, panel E, the scale bar shows mm divisions). Within the cyst-like structures H&E staining showed the formation of crude glomerulus-like structures (Figure 1, panels F and G). During development colonies demonstrated a characteristic epithelial cell “cobblestone” like morphology (Figure 1, panel H). At the time of use, podocyte-like cells exhibited the morphology of cultured podocytes, ie. large flat generally rounded cells with pronounced cytoskeleton (Figure 1, panel I).

Figure 2. Immunolabelling profiles of HIP, NHMC and AS1 podocyte-like cells at day 20 of differentiation. Images show high magnification images of single podocyte-like cells to confirm expression of podocyte markers; Wilms tumor-1 (WT1), and podocin (Nephrosis 2, Idiopathic, Steroid-Resistant protein). Images show representative cells from three different differentiations, except podocin in HIPs. Scale bar indicates 20μm (applicable to all images).

Figure 3. Effects of extracellular calcium ($[Ca^{2+}]_o$) on intracellular calcium ($[Ca^{2+}]_i$) in FURA-2AM loaded human immortalized podocyte-like cells. Panel (A) shows a typical effect of 2mM

JPET Fast Forward. Published on August 13, 2018 as DOI: 10.1124/jpet.118.250142
This article has not been copyedited and formatted. The final version may differ from this version.

$[Ca^{2+}]_o$ on fluorescence emission in one of 44 cells. The elevations of $[Ca^{2+}]_i$ induced by $[Ca^{2+}]_o$ could be mimicked by one calcium sensing receptor activator, spermidine, but not by another, gadolinium (Gd^{3+}). The effects of $[Ca^{2+}]_o$ appear elevated in the presence of NPS2143 (NPS, 10μM), a negative allosteric modulator of the calcium sensing receptor (panel B). In addition to elevations of $[Ca^{2+}]_i$, $[Ca^{2+}]_o$ and spermidine, but not Gd^{3+} also produced transient reductions in $[Ca^{2+}]_i$ (panel C). The effects of $[Ca^{2+}]_o$ on maximal elevations of $[Ca^{2+}]_i$ were not modulated by the large conductance calcium activated potassium channel inhibitor, iberiotoxin (100nM), nor by the voltage gated potassium channel blocker tetraethylammonium (TEA, 5mM, panel D). These potassium channels blockers had no effect upon the acute decreases in $[Ca^{2+}]_i$ elicited by $[Ca^{2+}]_o$ (panel E).

** and *** indicate significant differences (at $P<0.01$ and 0.001, respectively). Although data in panels (B)- (E) shows mean $\pm$ s.e. mean maximum or minimum responses expressed as a fraction of vehicle response, the statistical analysis compares responses of ligand with responses to vehicle control using one way ANOVA followed by post-hoc Dunnett's test. Data were analyzed using 44-97 cells (from four to seven replicate experiments) and expressed as a fraction of cell vehicle control.

Figure 4. Effects of extracellular calcium ($[Ca^{2+}]_o$) on intracellular calcium ($[Ca^{2+}]_i$) in FURA-2AM loaded normal human mesangial cell derived (NHMC) podocyte-like cells. Panel (A) shows a typical effect of 2mM $[Ca^{2+}]_o$ on fluorescence emission in one of 72 cells (six separate experiments). The elevations of $[Ca^{2+}]_i$ induced by $[Ca^{2+}]_o$ (panel B) could be mimicked by one calcium sensing receptor activator, spermidine (sperm), but not by another, gadolinium (Gd^{3+}). In addition to elevations of $[Ca^{2+}]_i$, $[Ca^{2+}]_o$ and spermidine, but not Gd^{3+} also produced transient

JPET Fast Forward. Published on August 13, 2018 as DOI: 10.1124/jpet.118.250142
This article has not been copyedited and formatted. The final version may differ from this version.

reductions in $[Ca^{2+}]_i$ (panel C). The effects of $[Ca^{2+}]_o$ on maximal elevations of $[Ca^{2+}]_i$ were not modulated by the large conductance calcium activated potassium channel inhibitor, iberiotoxin (100nM), the voltage gated potassium channel blocker tetraethylammonium (TEA, 5mM) or the focal adhesion kinase inhibitor, PF55271 (PF, 10nM, panel D). Both potassium channels blockers as well as the focal adhesion kinase inhibitor reversed the acute decreases in $[Ca^{2+}]_i$ elicited by $[Ca^{2+}]_o$ (panel E).

*** indicates significant differences ($P< 0.001$). Although data in panels (B)- (E) shows mean $\pm$ s.e. mean maximum or minimum responses expressed as a fraction of vehicle response, the statistical analysis compares responses of ligand with responses to vehicle control using one way ANOVA followed by post-hoc Dunnett's test. Data were analyzed using 53-107 cells (from four to seven replicate experiments) and expressed as a fraction of cell vehicle control.

Figure 5. Effects of extracellular calcium ($[Ca^{2+}]_o$) on intracellular calcium ($[Ca^{2+}]_i$) in FURA-2AM loaded Alport syndrome patient-derived podocyte-like cells (AS1). Panel (A) shows a typical effect of 2mM $[Ca^{2+}]_o$ on fluorescence emission in one of 31 cells (five separate experiments). The elevations of $[Ca^{2+}]_i$ induced by $[Ca^{2+}]_o$ could be mimicked by one calcium sensing receptor activator, spermidine, but not by another, gadolinium (Gd^{3+}), panel B. Neither spermidine, Gd^{3+} or $[Ca^{2+}]_o$ showed any transient reduction of $[Ca^{2+}]_i$ prior to elevation (panel C). The effects of $[Ca^{2+}]_o$ on maximal elevations of $[Ca^{2+}]_i$ were not modulated by the large conductance calcium activated potassium channel inhibitor, iberiotoxin (100nM), the voltage gated potassium channel blocker tetraethylammonium (TEA, 5mM) or the focal adhesion kinase inhibitor, PF55271 (PF, 10nM, panel D). The presence of the potassium channels blockers or PF did not promote the appearance of acute decreases in $[Ca^{2+}]_i$ elicited by $[Ca^{2+}]_o$ (panel E).

JPET Fast Forward. Published on August 13, 2018 as DOI: 10.1124/jpet.118.250142
This article has not been copyedited and formatted. The final version may differ from this version.

*** indicates significant differences (P< 0.001, one way ANOVA followed by post-hoc Dunnett's test). Data were analyzed using 31-103 cells (from five to seven replicate experiments) and expressed as a fraction of cell vehicle control.

Figure 6. Effects of extracellular calcium ($[Ca^{2+}]_o$) on intracellular calcium ($[Ca^{2+}]_i$) in FURA-2AM loaded Alport syndrome patient-derived podocyte-like cells (AS2). Panel (A) shows a typical effect of 2mM $[Ca^{2+}]_o$ on fluorescence emission in one of 47 cells (five separate experiments). The elevations of $[Ca^{2+}]_i$ induced by $[Ca^{2+}]_o$ (panel B) were not preceded by acute decreases in $[Ca^{2+}]_i$ (panel C).

*** indicates significant differences (P< 0.001, one way ANOVA followed by post-hoc Dunnett's test). Data was expressed as a fraction of cell vehicle controls.

Figure 7. Effects of a BKCa channel opener, NS1619 (1-10μM) on intracellular calcium. NS1619 promoted concentration-dependent decreases in $[Ca^{2+}]_i$ in NHMC and HIP, but not AS1 podocyte-like cells.

** and *** indicate significant differences (at P<0.01 and 0.001, respectively, one-way ANOVA followed by post-hoc Dunnett's test (n = 129 (NHMC), 48 (HIP) and 81 (AS1) cells from 7, 5 and 5 replicate experiments).

Figure 8. The effects of losartan and PD123,319 (both at 1μM) upon angiotensin II concentration-response effects in podocyte-like cells. Panels (A) to (D) respectively show responses to NHMC,

HIP, AS1 and AS2 podocyte-like cells. Responses of the three pluripotent stem cell derived lines could be uniformly blocked by the AT1 receptor antagonist, losartan.

* and ** indicate significant differences (at $P<0.05$ and 0.01, respectively, one-way ANOVA, n = 29-38 (NHMC), 30-38 (HIP), 34-49 (AS1) and 42-71 podocyte-like cells from four replicate experiments).

Figure 9. Immunolabelling of iPS derived NHMC and AS1 podocyte-like cells, as well as HIPs. Panels (A-C) respectively show DAPI, anti-KCNMA1 and phalloidin labelling of NHMC podocyte-like cells. Panels (D-F) respectively show DAPI, anti-KCNMA1 and phalloidin labelling of AS1 podocyte-like cells. Panels (G-I) respectively show DAPI, anti-KCNMA1 and phalloidin labelling of HIPs. Scale bar is 50μm.

Figure 10. Effects of re-plating AS1 podocyte-like cells either back onto (decellularized) plates that had contained either AS1 or NHMC podocyte-like cells. AS1 cells re-plated onto NHMC plates responded to low concentrations of extracellular calcium with acute reductions in intracellular calcium, an effect that could be blocked by the addition of tetraethylammonium (TEA, 5mM).

*** Indicates significant differences (at $P< 0.001$, respectively. Two way ANOVA with post-hoc Dunnett's test). Data was expressed as a fraction of vehicle control in 25-56 cells from four replicate experiments.

JPET Fast Forward. Published on August 13, 2018 as DOI: 10.1124/jpet.118.250142
This article has not been copyedited and formatted. The final version may differ from this version.

Figures

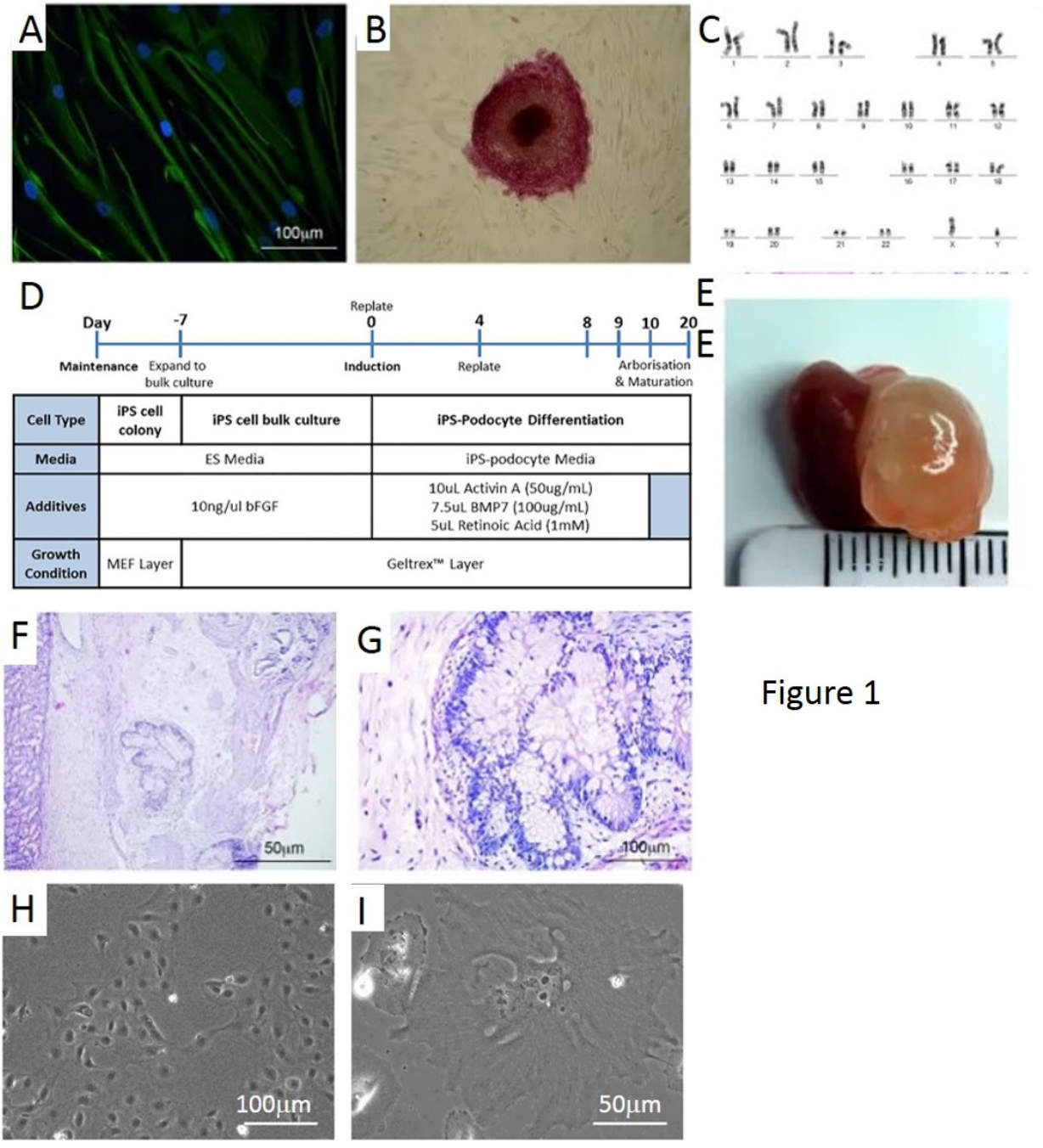

Figure 1

JPET Fast Forward. Published on August 13, 2018 as DOI: 10.1124/jpet.118.250142
This article has not been copyedited and formatted. The final version may differ from this version.

Figure 2

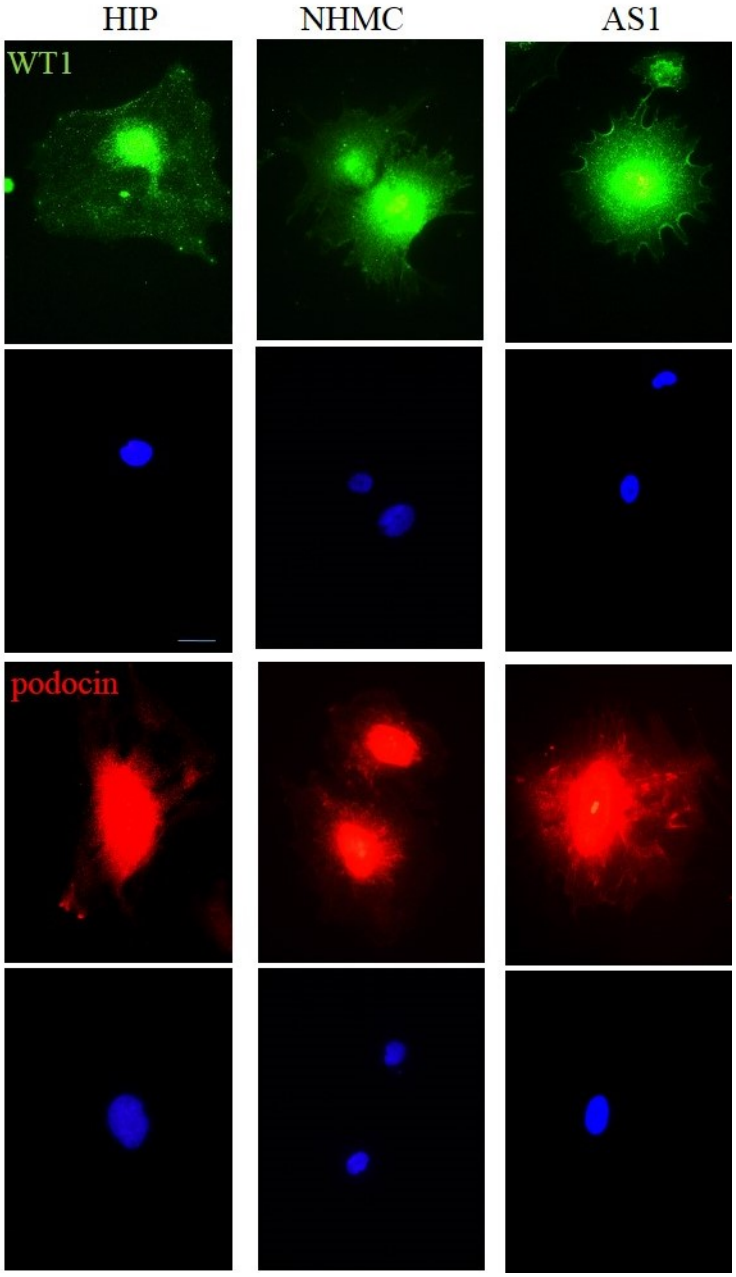

JPET Fast Forward. Published on August 13, 2018 as DOI: 10.1124/jpet.118.250142
This article has not been copyedited and formatted. The final version may differ from this version.

Figure 3

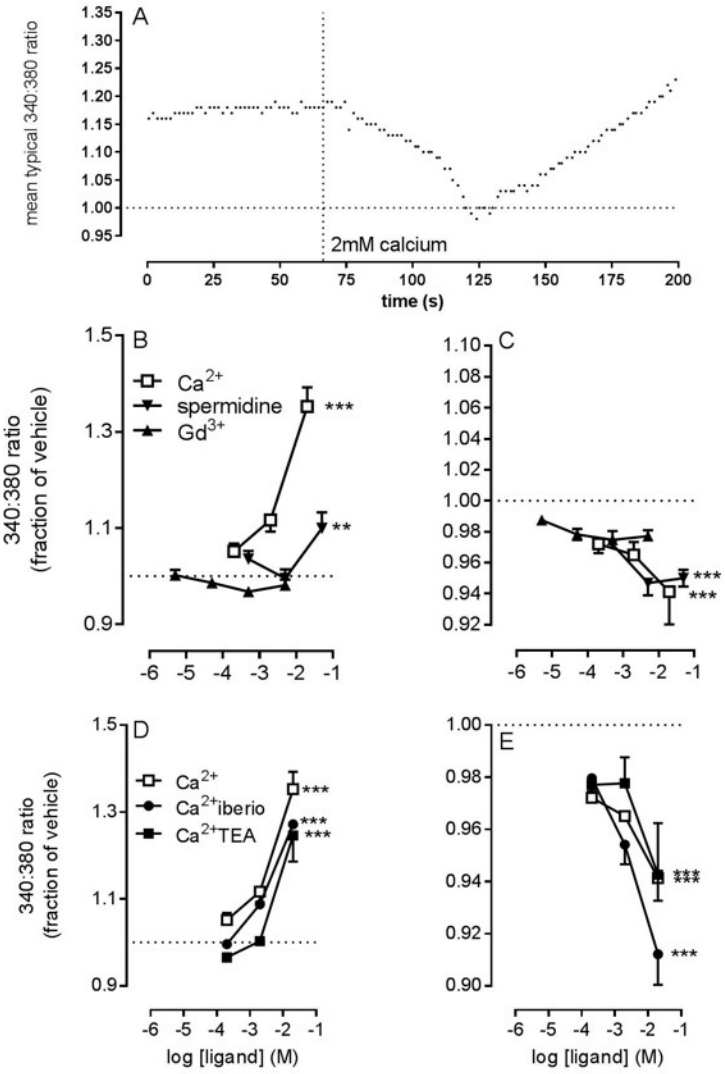

JPET Fast Forward. Published on August 13, 2018 as DOI: 10.1124/jpet.118.250142
This article has not been copyedited and formatted. The final version may differ from this version.

Figure 4

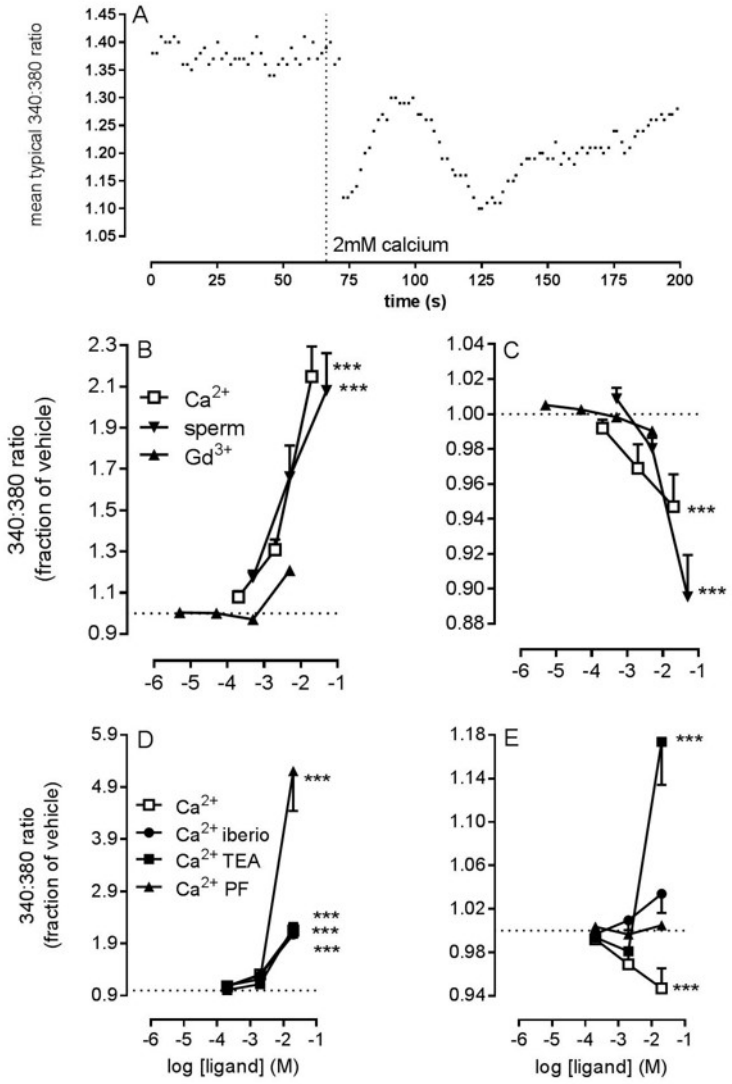

JPET Fast Forward. Published on August 13, 2018 as DOI: 10.1124/jpet.118.250142
This article has not been copyedited and formatted. The final version may differ from this version.

Figure 5

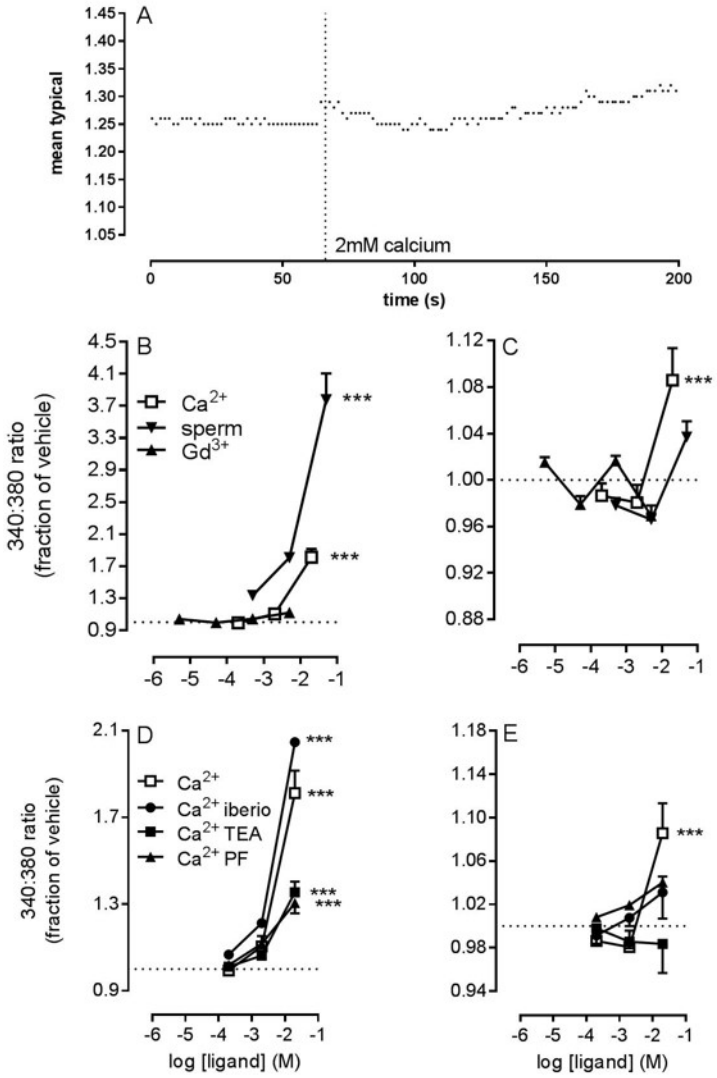

JPET Fast Forward. Published on August 13, 2018 as DOI: 10.1124/jpet.118.250142
This article has not been copyedited and formatted. The final version may differ from this version.

Figure 6

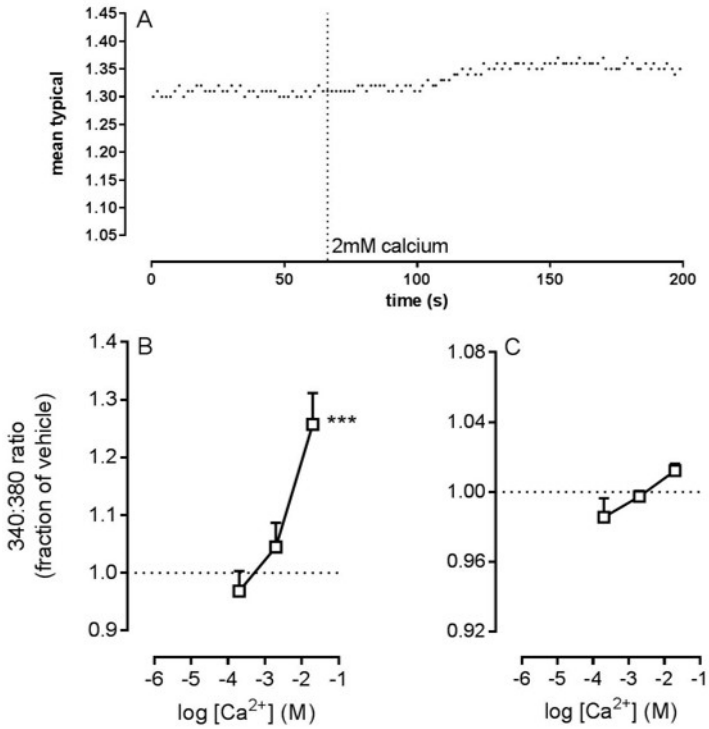

JPET Fast Forward. Published on August 13, 2018 as DOI: 10.1124/jpet.118.250142
This article has not been copyedited and formatted. The final version may differ from this version.

Figure 7

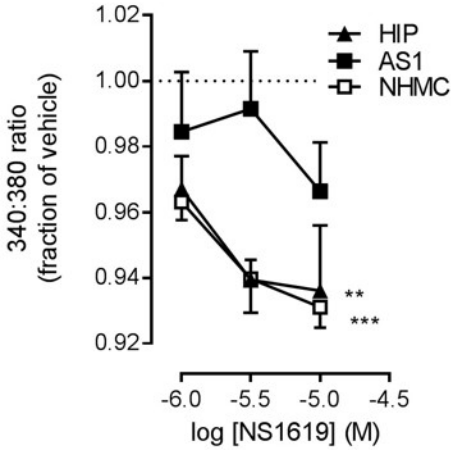

Figure 8

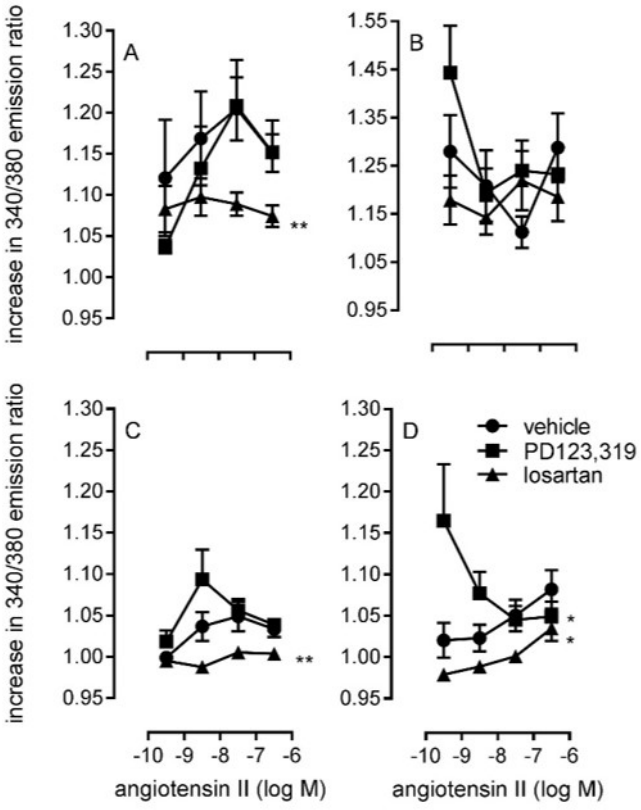

JPET Fast Forward. Published on August 13, 2018 as DOI: 10.1124/jpet.118.250142
This article has not been copyedited and formatted. The final version may differ from this version.

Figure 9

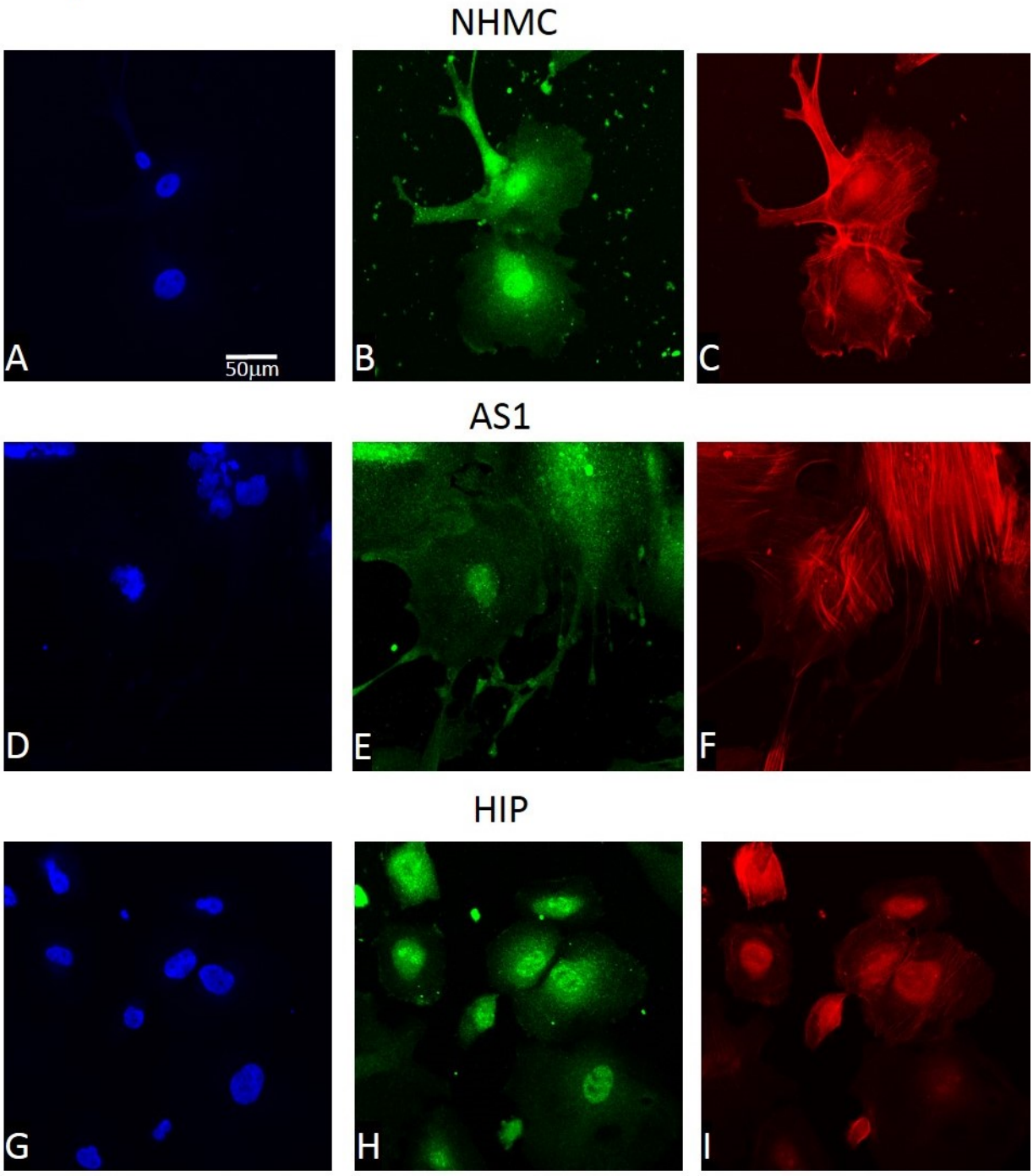

JPET Fast Forward. Published on August 13, 2018 as DOI: 10.1124/jpet.118.250142
This article has not been copyedited and formatted. The final version may differ from this version.

Figure 10